Asian Journal of Chemistry; Vol. 38, No. 4 (2026), 901-908
ASIAN JOURNAL OF CHEMISTRY
https://doi.org/10.14233/ajchem.2026.35131

Synthesis of Fluorescent N,P doped Carbon Quantum Dots Based Test Strip for Onsite Detection of Tartrazine and Ascorbic Acid

G. RUBY and P. BHAVANI*

PG and Research Department of Chemistry, R.V. Government Arts College, Chengalpattu-603001, India

*Corresponding author: E-mail: bhavaniperumal4@gmail.com

Received: 19 October 2025 *Accepted*: 2 February 2026 *Published online*: 8 April 2026 AJC-22311

Tartrazine and ascorbic acid are the prevalent food additives whose excessive use may lead to health complications, including allergies, behavioural alterations and oxidative stress. Expeditious, economical and dependable detection technologies are crucial for ensuring food safety and safeguarding customers. In this work, nitrogen and phosphorus co-doped carbon quantum dots (N,P-CQDs) were easily synthesized in one step *via* hydrothermal treatment of citric acid and ammonium phosphate. The fluorescent N,P-CQDs were immobilized on Whatman filter paper to create portable test strips for detecting tartrazine and ascorbic acid. Fluorescence quenching under UV light, due to photoinduced electron transfer and complex formation, enabled sensitive, selective and rapid detection within 3 min. The strips are stable, reusable and user-friendly, offering a practical approach for on-site beverage screening without complex instruments.

Keywords: Tartrazine, Ascorbic acid, Carbon quantum dots, Beverages analysis, Food safety.

INTRODUCTION

Tartrazine is a synthetic lemon-yellow azo dye extensively utilized to colour carbonated beverages, confections and processed foods owing to its solubility in water and economic viability. Ascorbic acid, a natural antioxidant, is frequently used as a preservative and nutritional supplement [1], enhancing immune function and skin health in vitamin-fortified goods. While both tartrazine and ascorbic acid are generally renowned as safe by food safety authorities such as the United States Food and Drug Administration (USFDA) and the European Food Safety Authority (EFSA) [2,3]. Excessive intake can lead to potential health concerns. Numerous clinical and epidemiological studies indicated that overconsumption of tartrazine may cause hyperactivity, migraines, asthma and urticaria [4]. As a result, the use of tartrazine is strictly regulated with acceptable limits. Similarly, ascorbic acid though essential can act as a pro-oxidant in high concentrations especially in the presence of metal ions like iron or copper leading to oxidative stress and cellular damage. Therefore, specific monitoring of these additives in beverages is essential for public health assurance [5].

Traditional analytical methods for detecting tartrazine and ascorbic acid include high-performance liquid chromatography (HPLC), UV-visible spectrophotometry and electrochemical sensors are reported [6-8]. Although these approaches provide exceptional sensitivity and selectivity, they need expensive apparatus, skilled personnel and complex sample preparation processes [9]. Consequently, they are unsuitable for rapid and on-site screening, which is increasingly required in food safety standards and quality control. This has stimulated the advancement of new detection methods that are portable, economical and user-friendly, while maintaining the accurate analytical efficacy.

Fluorescent carbon quantum dots have emerged as an attractive option in this regard. Among diverse nanomaterials, carbon quantum dots (CQDs) have attracted considerable interest owing to their remarkable optical characteristics, biocompatibility, aqueous solubility and chemical tunability. These quasi-spherical nanoparticles, generally measuring under 10 nm, display distinctive photoluminescence properties, such as adjustable emission wavelengths, elevated quantum yield and superior photostability. Furthermore, their surfaces can be easily modified with heteroatoms like nitrogen, phosphorus, sulfur, and oxygen to improve selectivity, sensitivity and interaction with target analytes. These changes can markedly enhance the electron-donating or -accepting characteristics, hence promoting specific binding or quenching interactions with certain molecules [10].

Nitrogen- and phosphorus-co-doped carbon quantum dots (N,P-CQDs) have attracted attention for fluorescence-based sensing applications. Nitrogen doping enhances the quantum yield and surface defects that improve fluorescence properties, while phosphorus doping modifies the electronic structure and introduces active binding sites [11]. The combined effect of these dopants improves charge transfer and analyte interaction, making N,P-CQDs suitable for detecting compounds such as azo dyes and antioxidants. Application to commercial beverages such as soft drinks, vitamin-enriched water and fruit juices produced high recovery values with results comparable to UV-visible spectrophotometric analysis [12,13].

The ease of use, low production cost, high sensitivity and selectivity of the developed test strips make them highly attractive for regulatory system, food manufacturers and consumers seeking an accessible method for food quality assurance. This platform eliminates the need for centralised laboratories or skilled personnel making it ideal for employment in remote or resource constrained environments [14]. Moreover, the fluorescence-based sensor detection visible under simple handheld UV lamp even non-experts to understand the results [15,16]. Thus, to develop easy real-world application and on-field usability, the CQDs were immobilised onto cellulose-based filter paper to make test strips. These strips allow fast visual detection of the analytes without the need for instrumentation. When the test strip is dipped into a sample, the interaction between the analytes and the surface functional groups of photo-induced electron transfer (PET) and complexation mechanisms, where the conjugated structures of tartrazine and the redox activity of sample affect the electron density of the CQDs leading to a decrease in emission intensity [17].

In this study, a fluorescence-based test strip incorporating N,P-CQDs was developed for the selective detection of tartarzine and ascorbic acid in beverage samples. The CQDs were synthesized *via* a hydrothermal method using citric acid as carbon precursor and ammonium phosphate as nitrogen and phosphorus source.

EXPERIMENTAL

Citric acid ($C_6H_8O_7$) and ammonium hydrogen phosphate ($(NH_4)_2HPO_4$) were used for the primary carbon, nitrogen and phosphorus sources for the synthesis of N,P-doped carbon quantum dots (N,P-CQDs). Tartrazine (E102) and ascorbic acid both are the target analyte and Whatman filter paper (Grade 1) for making the test strips. Deionised water was used for the synthesis and experimental procedures to avoid contamination.

Synthesis of N,P-CQDs: N,P-CQDs were synthesised *via* a hydrothermal method. Briefly, 2 g of citric acid and 1 g of ammonium hydrogen phosphate were dissolved in 30 mL of deionised water followed by stirred for 10 min to obtain clear solution. The solution was transferred into a 50 mL Teflon-lined autoclave and heated at 180 ºC for 6 h. After cooling to room temperature, the colour of the solution turned dark yellow-brown solution confirmed the formation of N,P-CQDs. Then, it was dialysed against deionised water for 24 h to remove impurities. The final N,P-CQDs solution was stored at 4 ºC for further use.

Quantum yield: The quantum yield (QY) of synthesised N,P-CQDs was calculated by quinine sulphate in 0.1 M H_2SO_4 (QY = 0.54) using the following equation:

$$QY_{sample} = QY_{ref} \times \left(\frac{I_{sample}}{I_{ref}}\right) \times \left(\frac{A_{ref}}{A_{sample}}\right) \times \left(\frac{\eta_{sample}}{\eta_{ref}^{2}}\right)$$

where I = the integrated fluorescence intensity, A = the absorbance at excitation wavelength, η = refer to the refractive index of sample

Based on this method, the calculated quantum yield of N,P-CQDs was 18.2%.

Characterisation: The nanoscale dimensions of N,P-CQDs were verified by analyzing the morphology and particle size distribution using transmission electron microscopy (TEM, FEI Tecnai G2 20 TEM instrument). Fourier transform infrared (FTIR) spectroscopy (Nicolet iS10) was used to identify the surface functional groups. The characteristic absorption peaks of CQDs was identified by the UV-Visible absorption spectroscopy (Shimadzu UV-2600 UV-Vis spectrophotometer). The functionality and effectiveness of carbon quantum dots-based sensors was acknowledged by photoluminescence (PL, Horiba Fluoromax-4 spectrofluorometer). X-ray photoelectron spectroscopy (JEOL JPS-9030) was used to investigate the elemental composition and bonding states of CQDs. Zeta potential (Malvern Instruments, U.K.) was used to assess the surface charge and colloidal stability of the synthesised CQDs. Fluorescence lifetime spectroscopy (Edinburgh Instruments FLS1000 (TCSPC module), U.K.) was employed to find out the excited state of carbon quantum dots and their interaction mechanism with additives.

Detection of tartrazine and ascorbic acid: The synthesised N,P-CQDs exhibited strong blue fluorescence properties under UV lamp, which was effectively modulated to detect tartrazine and ascorbic acid. Moreover, the addition of tartarzine and ascorbic acid to the N,P-CQDs solution buffered with PBS (pH 7.4), a significant decrease in fluorescence intensity was observed indicated of a quenching mechanism. For sensing experiments, 50 μL of N,P-CQDs and 1 mL of PBS were introduced by the addition of varying concentrations of tartrazine (0.1 to 10 μM) or ascorbic acid (0.2 to 12 μM). The solutions were incubated for 15 min at room temperature to allow sufficient interaction. The fluorescence properties of N,P-CQDs were recorded at an excitation wavelength of 350 nm and emission was monitored at 430 nm.

Preparation for real samples: To estimate the practical applicability of the developed N,P-CQDs based fluorescent test strips on real beverage samples such as soft drinks, fruit juices and energy drinks were collected from the local markets. Earlier to analysis the samples underwent a simple pretreatment to remove particulate matter and minimize matrix effects. Each beverage sample (5 mL) underwent ultrasonic degassing for 10 min to expel dissolved gases and reduce foaming, then followed by filtration to remove suspended particulates. The filtered sample was subsequently diluted 10-folds with phosphate-buffered saline (pH 7.4) to adjust analyte concentrations to the sensor's linear detection range. The pretreatment samples were either directly put to the N,P-CQDs test strips or examined by cuvette-based fluorescence measurements. To

validate, established concentrations of tartrazine and ascorbic acid were introduced into chosen samples to assess recovery efficiency and possible matrix interference.

RESULTS AND DISCUSSION

FTIR studies: Fig. 1 illustrates the FTIR spectra of the synthesised CQDs and their precursor. The carboxylic functional group at 3455 cm^{-1} and amide stretching vibration at 3146 were clearly identified [18,19]. A sharp peak at 1653 cm^{-1} indicates the carbonyl stretching frequency of amide in FTIR spectra of CQDs. After carbonisation changing of the sharp peak of carbonyl stretching frequency of carboxylic functionality of citric acid at 1725 cm^{-1} to the carbonyl stretching frequency of amide in FTIR spectrum of CQDs confirmed the formation of amide linkage on the surface of the CQDs. Simultaneously the peaks at 1400 cm^{-1} and 1078 cm^{-1} indicate the bending vibration of the N–H bond and stretching vibration of the C–N bond [20,21]. In the FTIR spectrum of ammonium hydrogen phosphate, the peaks at 1100 cm^{-1} and 550 cm^{-1} can be assigned to the stretching vibration of phosphate groups. After the formation of CQDs significant decrease in the intensity of the bands at 550 cm^{-1} and 1100 cm^{-1} are observed, which indicates the presence of phosphorus in the CQDs. These diverse surface groups not only contribute to the high fluorescence quantum yield and environmental stability of the CQDs. But also play a key role in the selective interaction with tartrazine through electrostatic forces, hydrogen bonding and π–π stacking [22,23]. Therefore, FTIR analysis confirms that the hydrothermal synthesis route effectively introduces N,P-doped carbon matrix resulting in highly functionalised and reactive CQDs suitable for fluorescence based sensing applications.

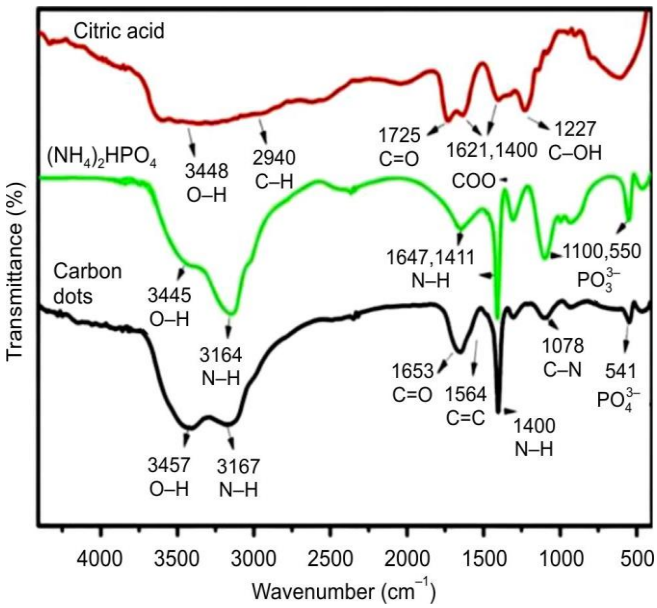

Fig. 1. FITR spectra of citric acid, ammonium hydrogen phosphate and synthesised N,P-CQDs

XPS studies: The XPS analysis was taken to identify the surface functional state, components and successful doping of the synthesised N,P-CQDs confirms the presence of carbon, nitrogen, phosphorus and oxygen as the main elements. The XPS spectrum (Fig. 2a) displays distinct peaks corresponding to C_{1s} (~285 eV), N_{1s} (~400 eV) and O_{1s} (~532 eV) verifying the elemental composition [24]. The high-resolution C_{1s} spectrum (Fig. 2b) can be deconvoluted into four peaks assigned to C–C, C=C (284.73 eV), C–N, C-P (286.28 eV) indicating the pre-sence of carbon, nitrogen and phosphorus doping containing groups.

The N_{1s} spectrum (Fig. 2c) exhibits two peaks. The peak at approximately 399.0 eV corresponds to the =NH– group, while the peak at around 400.3 eV is attributed to N–C and N–H bonds, confirming the successful incorporation of nitrogen into the carbon-dot structure in multiple bonding environments. This incorporation enhances the electronic properties of the material and contributes to improved fluorescence and sensing performance [25,26]. Similarly, the P_{2p} spectrum (Fig. 2d) displays the characteristic peaks corresponding to P=O (≈132.83 eV), P–C/P–N (≈133.54 eV) and P–O (≈134.98 eV), indicating the presence of the functional groups. These heteroatom-containing functional groups improve electronic properties, fluorescence behaviour and surface reactivity of the N,P-CQDs, making them suitable for sensing applications [27].

UV-Visible absorption studies: The UV-visible absorption spectrum shows two distinct absorption bands *viz*. a strong band below 250 nm and another in the 320-350 nm region (Fig. 3). The lower wavelength band is attributed to π→π* transitions associated with C=C bonds or aromatic domains in the carbon framework, while the band in the near-UV region corresponds to n→π* or charge-transfer transitions related to the surface functional groups [28].

Nitrogen and phosphorus incorporation into the carbon matrix introduces defect states and additional surface functionalities, resulting in the modifications to the electronic structure of the CQDs. This leads to broadened optical absorption and improved excitation-dependent fluorescence behaviour [29]. Such optical characteristics are important for selecting appropriate excitation wavelengths in photoluminescence studies and support the applicability of N,P-CQDs in fluorescence-based sensing of contaminants such as tartrazine through quenching mechanisms [30].

Fluorescence studies: Upon excitation by light at 360 nm, the N,P-CQDs exhibit strong fluorescence emission commonly centered around 440-450 nm exhibiting a characteristic blue luminescence (Fig. 4a-d). This fluorescence arises from the excitons where electrons excited state to the ground state emitting photons in the process. The emission properties of N,P-CQDs are significantly influenced by the presence of surface defects, functional groups and the heteroatom doping of nitrogen and phosphorus. Nitrogen atoms introduced surface states and active sites to improve fluorescence quantum yield [31]. This tunable fluorescence behaviour is beneficial for multi-colour imaging and sensing. Moreover, the fluorescence of N,P-CQDs is stable across a broad pH range and exhibits good photostability, which is advantageous for practical applications [32]. Thus, fluorescence spectroscopy not only characterizes the optical features of N,P-CQDs but also underpins their function in chemical and biological sensing.

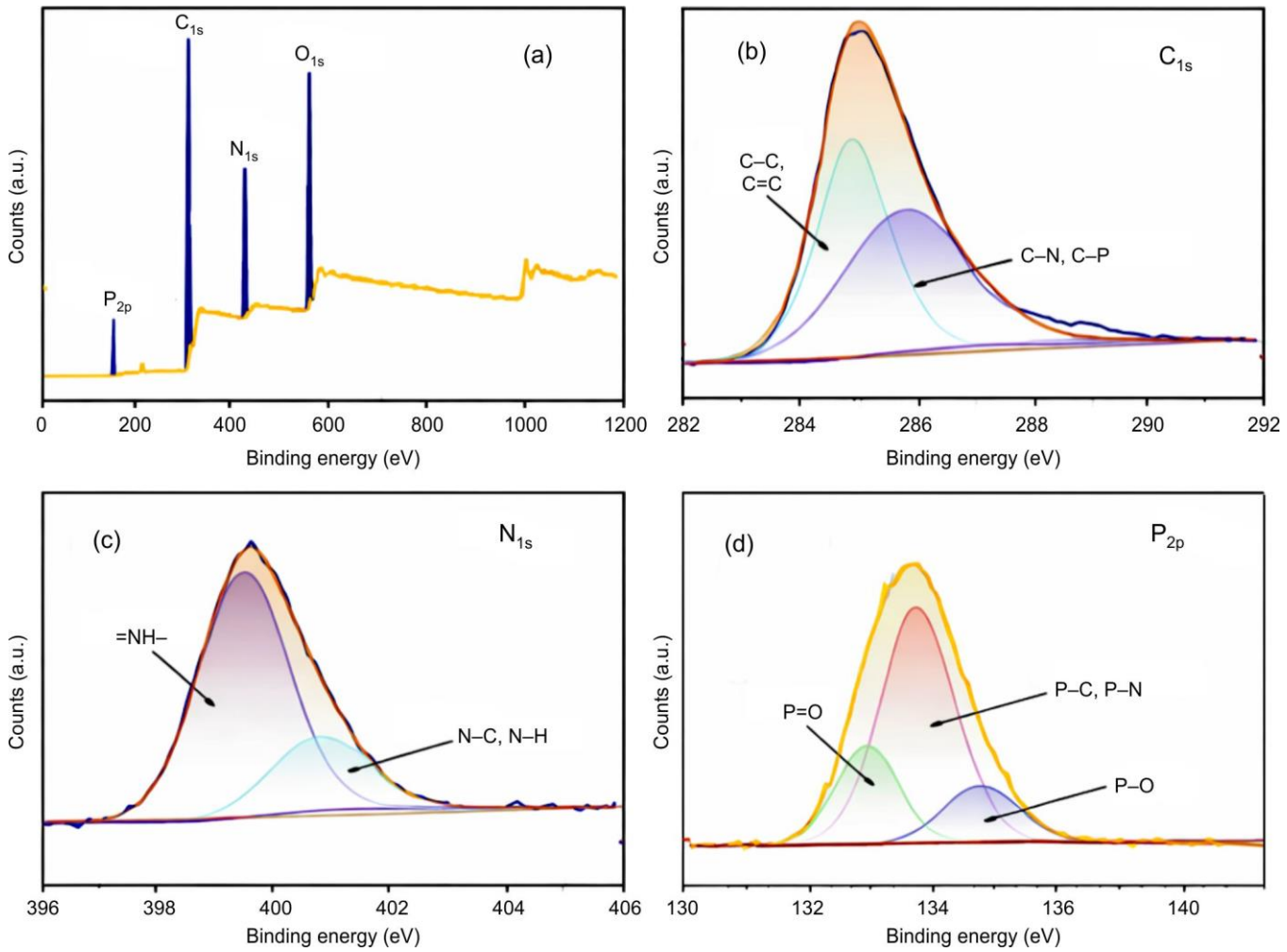

Fig. 2. XPS spectra of N,P-CQDs: (a) survey scan, (b) C_{1s}, (c) N_{1s} and (d) P_{2p} demonstrating the surface functional groups and elemental distributions

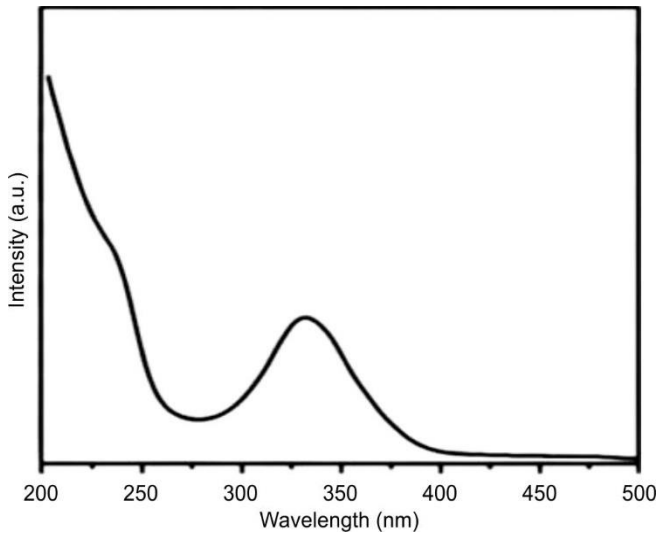

Fig. 3. UV-visible spectrum of N,P-CQDs

To evaluate the fluorescence sensing capability of the synthesised N,P doped carbon quantum dots (N,P-CQDs) the quenching of photoluminescence (PL) intensity was systematically studied in the presence of varying concentrations of tartrazine and ascorbic acid. The fluorescence responses were recorded at 440 nm with F and F_0 representing the PL intensity in the presence and absence of the analytes, respectively. The F/F_0 plot expose a decrease in fluorescence intensity upon the addition of both tartrazine and ascorbic acid with the remarkably stronger quenching observed for tartrazine compared to ascorbic acid. The presence of tartrazine efficiently quenched the PL emission of N,P-CQDs suggesting a sensitive interaction due to π–π stacking interactions between the aromatic rings of tartrazine and the conjugated structure of CQDs along with possible hydrogen bonding with surface functional groups. In case of ascorbic acid, the quenching effect is attributed to its strong reducing nature which promotes electron transfer from ascorbic acid to the excited state of CQDs [33]. A continuous decrease in the fluorescence intensity was observed with increasing concentrations of tartrazine and ascorbic acid as depicted in Fig. 5a-b. The inset of Fig. 5c-d shows the plot of $(F_0\text{-}F)/F_0$ *versus* analyte concentration, which demonstrates a linear relationship in the concentration range of 0-1000 μM for tartrazine ($R^2 = 0.998$) and 0-1300 μM for ascorbic acid ($R^2 = 0.987$) confirming the potential of N,P-CQDs as an effective fluorescent sensor for detecting tartrazine and ascorbic acid with high sensitivity.

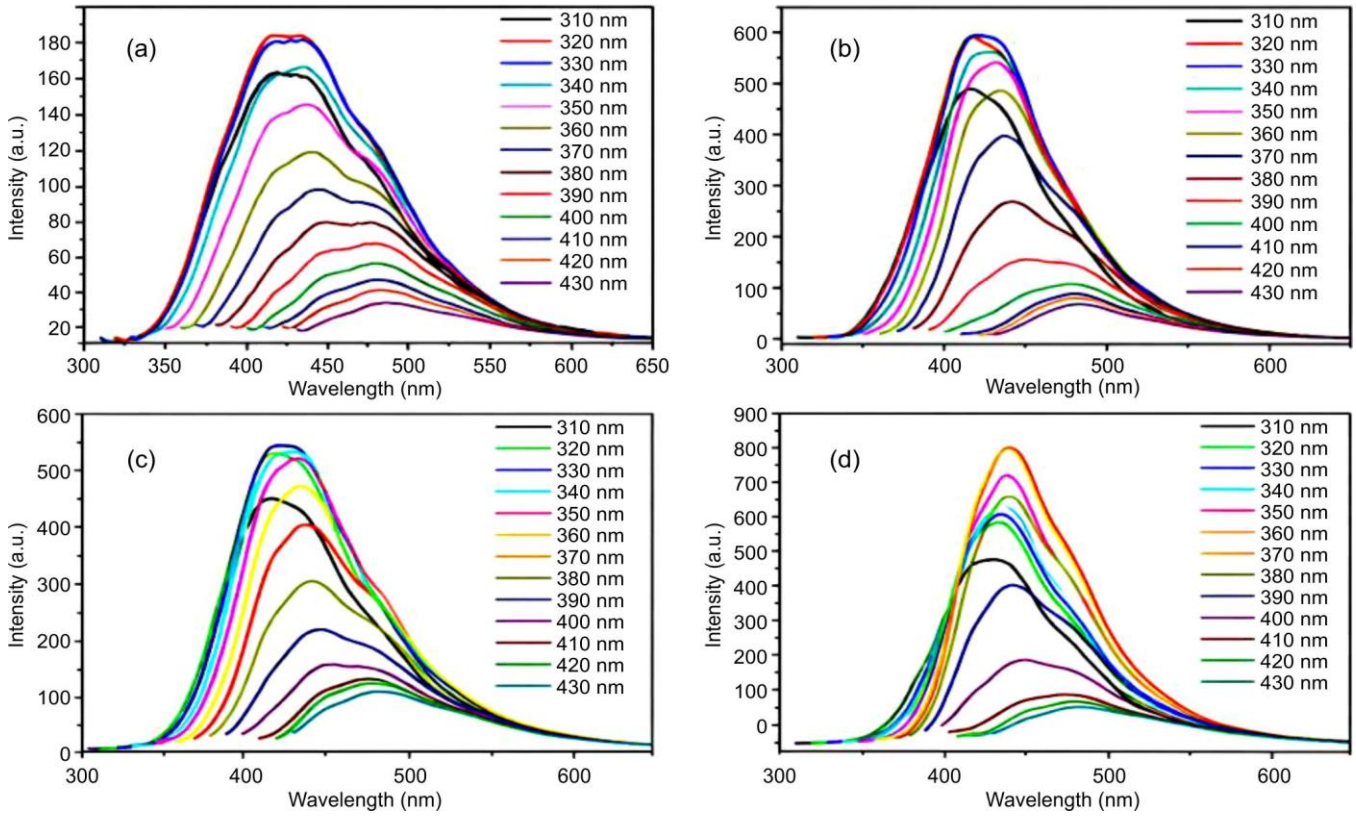

Fig. 4. Photoluminescence spectra of the N,P-CQDs synthesised from citric acid and diammonium hydrogen phosphate (a) 1:1, (b) 1:2, (c) 1:3 and (d) 1:4 ratio at different excitations

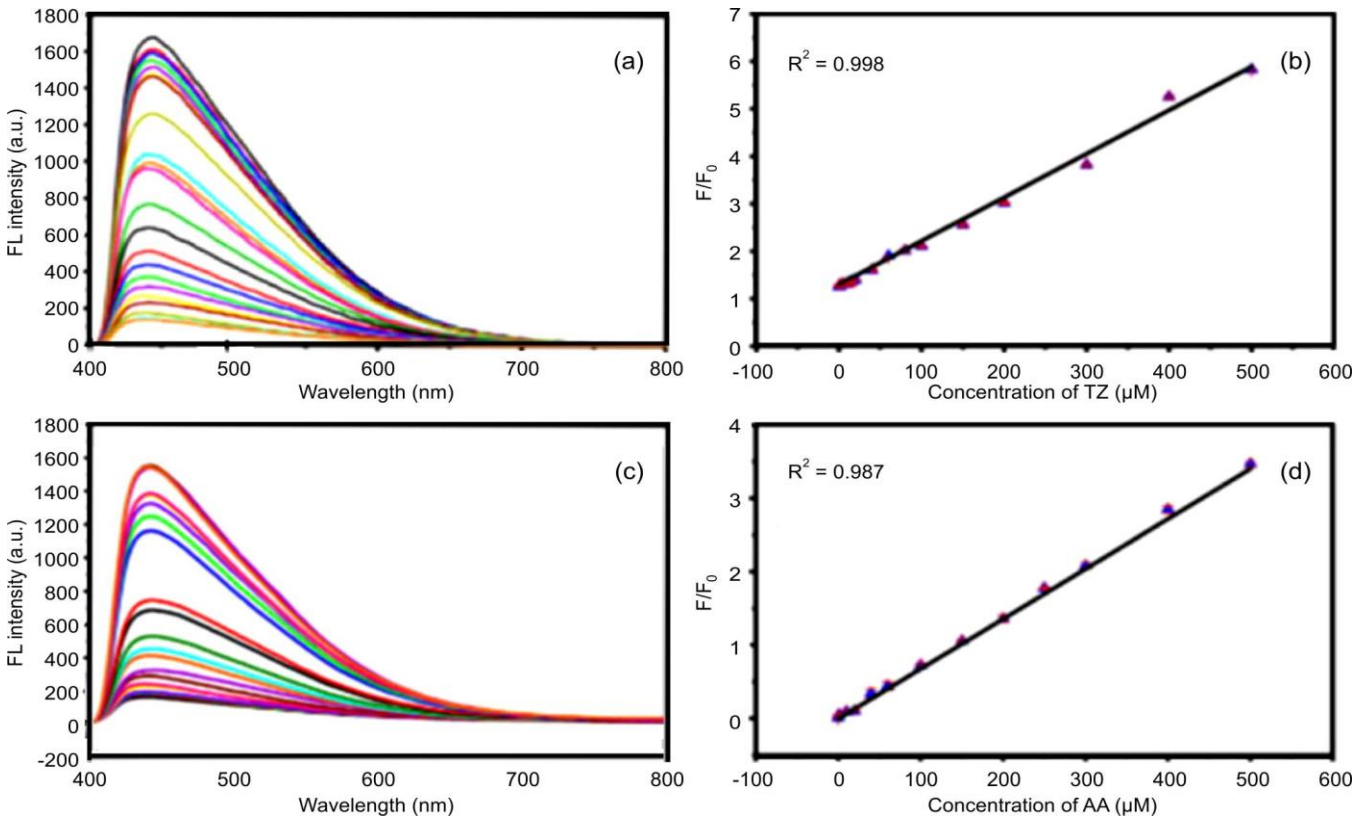

Fig. 5. (a) Fluorescence emission spectra of N,P-CQDs with different concentrations of tartrazine, (b) calibration plot of F_0/F *vs.* concentration of tartrazine, (c) Fluorescence emission spectra of N,P-CQDs with different concentrations of ascorbic acid, and (d) calibration plot of F_0/F *vs.* concentration of ascorbic acid

TEM studies: The synthesized N,P-CQDs show a quasi-spherical particles with uniform distribution. The HRTEM images showed clear lattice fringes with an interplanar spacing confirmed the spherical morphology as well as uniform particle size (Fig. 6). There is no diffraction phase observed in the selected area electron diffraction (SAED) pattern of carbon quantum dots corresponded to the N,P-CQDs reflected the poor crystalline structure of the carbon dots. The weak diffraction spots indicate the presence of crystalline domains in the N,P-CQDs, which further corroborate successful N and P doping. The size-distribution histogram of the N,P-CQDs, obtained from TEM image analysis, shows a narrow particle-size distribution with an average diameter of 4.5 nm, indicating uniform dispersion (Fig. 6d). This uniformity is beneficial for maintaining the consistent optical properties, particularly fluorescence behaviour. Moreover, the well scattered N,P-CQDs were confirmed their high colloidal stability in aqueous medium [34].

Sensitivity and selectivity: The sensitivity and selectivity of the test strips of nitrogen and phosphorus doped carbon quantum dots (N,P-CQDs) for the detection of tartrazine and ascorbic acid were evaluated by fluorescence quenching measurements. The test strips exhibited a clear and linear fluorescence quenching response to increasing concentrations of both tartrazine and ascorbic acid with measurable detection ranges between 0.5 to 50 μM. The calculated detection limit for tartrazine was 0.15 μM while ascorbic acid was low indicating high sensitivity for both analytes even at trace level relevant in food and beverages [35]. The selectivity of the test strips was further confirmed by testing in the presence of other common beverage components such as glucose, citric acid and food colourants. These substances caused for the detection of tartrazine and ascorbic acid by the fluorescence quenching mechanism was predominantly is shown Fig. 7. This dual detection capability combined with high sensitivity and selectivity makes the N,P-CQDs based test strips highly effective for the rapid and on-site monitoring of tartrazine and ascorbic acid in commercial beverages contributing to improved food quality control and safety assessments.

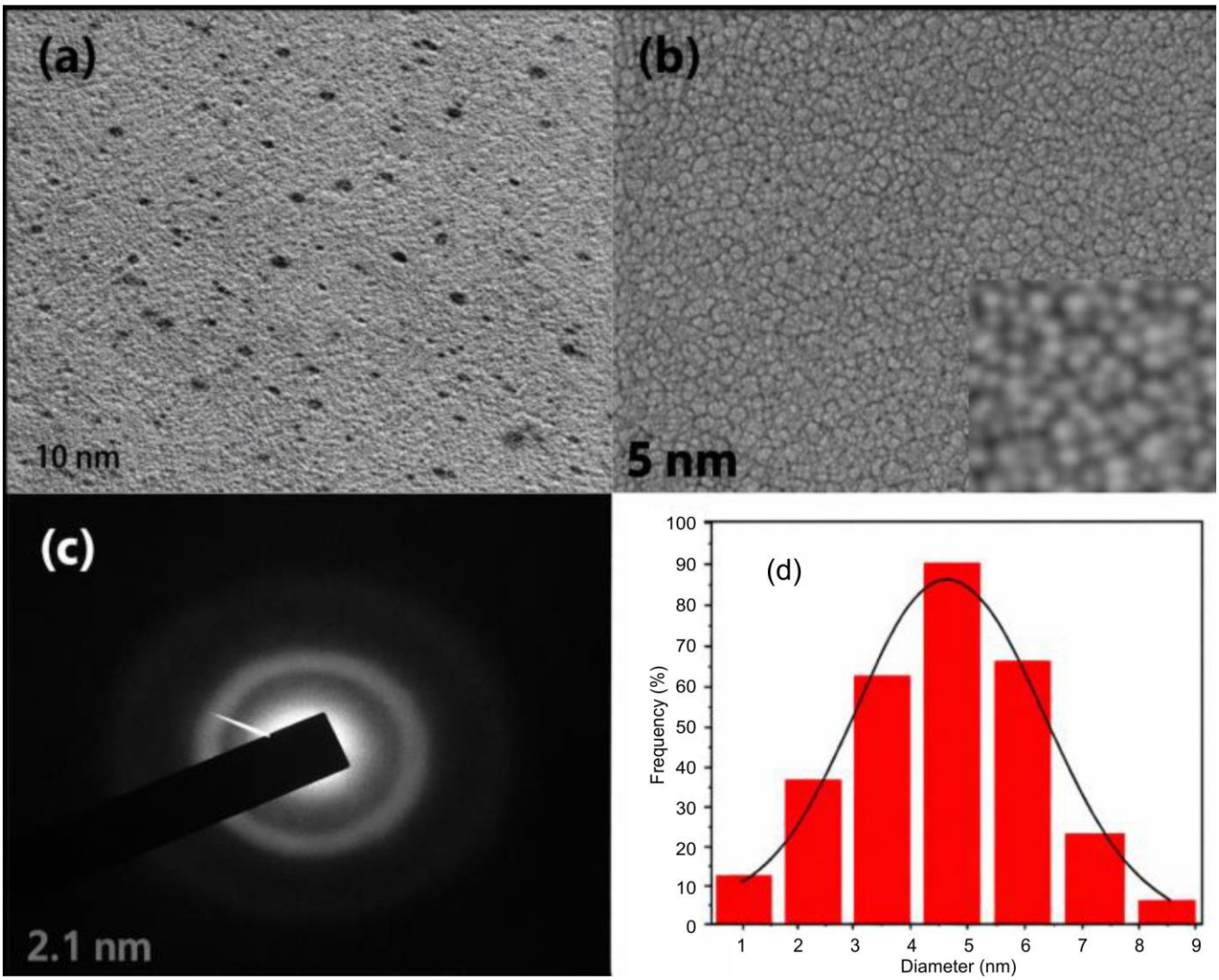

Fig. 6. (a) TEM image reveals that N,P-CQDs are uniformly dispersed, (b) HR-TEM image shows clear lattice fringes which confirm the crystalline character of N,P-CQDs, (c) SAED pattern demonstrates the crystalline nature of N,P-CQDs, and (d) Particle size distribution analysis of N,P-CQDs

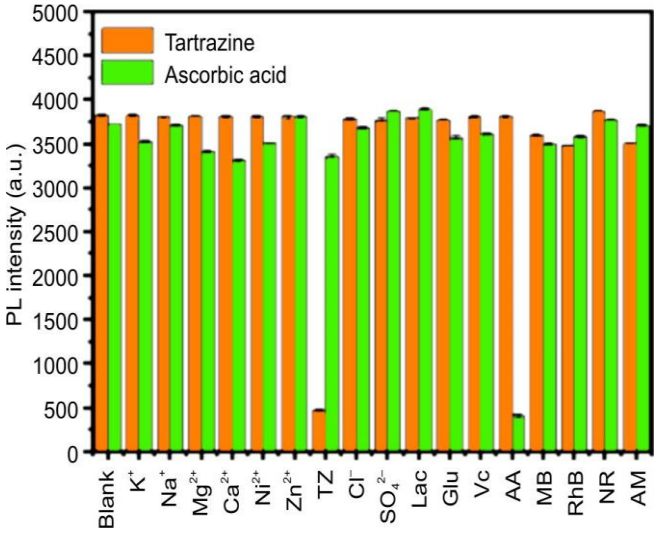

Fig. 7. Selectivity and interference study showing the relative fluorescence response for tartrazine (orange bars) and ascorbic acid (green bars) in the presence of various potential interfering substances

Stability and practical application: The stability and practical application of the N,P-CQDs based fluorescent test strips were evaluated for the detection of both tartrazine and ascorbic acid in real world scenarios [36,37]. The test strips exhibited (pH range of 4 to 10) fluorescence intensity without significant degradation. For practical application, the test strips were evaluated on a variety of commercial soft drinks and fruit juices to detect both tartrazine and ascorbic acid. The analysis yields high recovery rates ranging from 81.2% to 90.7% for both analytes (Tables 1 and 2). These findings confirm that the N,P-CQDs based test strips are robust, versatile and effective for on-site detection of tartrazine and ascorbic acid contributing to enhanced food safety monitoring and quality control with minimum technical requirements.

TABLE-1
DETERMINATION OF TARTRAZINE IN DIFFERENT BEVERAGES WITH THE PROPOSED METHOD

Sample	Beverage type	Measured tartrazine (mg/L)	Recovery (%)	RSD (%)
S1	Orange soda	12.8 ± 0.3	97.5	2.4
S2	Mango juice	9.7 ± 0.2	95.8	2.1
S3	Pineapple juice	7.3 ± 0.1	99.2	1.8
S4	Mango juice	ND	–	–

ND = Non-detectable or below the limit of detection (0.02 μM).
RSD = Relative standard deviation.

TABLE-2
DETERMINATION OF ASCORBIC ACID IN DIFFERENT BEVERAGES WITH THE PROPOSED METHOD

Sample	Beverage type	Measured ascorbic acid (mg/L)	Recovery (%)	RSD (%)
S1	Mixed fruit juice	31.6 ± 0.5	97.5	2.4
S2	Orange juice	45.1 ± 0.7	95.8	2.1
S3	Lemon soda	25.3 ± 0.4	99.2	1.8
S4	Apple drink	18.9 ± 0.3	99.5	1.2

RSD = Relative standard deviation.

Conclusion

This work presents the nitrogen and phosphorus doped carbon quantum dots (N,P-CQDs) based fluorescent test strip. It is simple, cost-effective and portable test strip for the dual detection of tartrazine and ascorbic acid in beverages. The test strip utilizes the strong fluorescence properties of N,P-CQDs which undergo significant quenching in the presence of both tartrazine and ascorbic acid enabling visual detection under UV light. The sensor demonstrates high sensitivity with a low detection limit of 0.12 μM for tartrazine and comparable sensitivity for ascorbic acid along with a linear response across a broad concentration range for both analytes. This allows for accurate quantification even at trace levels usually found in commercial beverages. The test strip exhibits excellent selectivity showing minimum interference from other common beverage ingredients such as glucose, citric acid and additional food colourants. Furthermore, it maintains stability under varying pH conditions and temperatures enhancing its reliability for practical use. These features make the N,P-CQDs based test strip a hopeful tool for point of care testing and on-site monitoring of tartrazine and ascorbic acid especially in resource limited settings where quick, reliable and simultaneous detection is crucial for ensuring food safety and quality control.

CONFLICT OF INTEREST

The authors declare that there is no conflict of interests regarding the publication of this article.

DECLARATION OF AI-ASSISTED TECHNOLOGIES

During the preparation of this manuscript, the authors used an AI-assisted tool(s) to improve the language. The authors reviewed and edited the content and take full responsibility for the published work.

REFERENCES

1. H. Li, X. He, Z. Kang, H. Huang, Y. Liu, J. Liu, S. Lian, C.H.A. Tsang, X. Yang and S.-T. Lee, *Angew. Chem. Int. Ed.*, **49**, 4430 (2010); https://doi.org/10.1002/anie.200906154
2. P. Amchova, F. Siska and J. Ruda-Kucerova, *Heliyon*, **10**, e38111 (2024); https://doi.org/10.1016/j.heliyon.2024.e38111
3. M. Bastaki, T. Farrell, S. Bhusari, K. Pant and R. Kulkarni, *Food Chem. Toxicol.*, **105**, 278 (2017); https://doi.org/10.1016/j.fct.2017.04.034
4. Y. Nie, J. Guo, Y. Deng and W. Weng, *J. Saudi Chem. Soc.*, **24**, 865 (2020); https://doi.org/10.1016/j.jscs.2020.09.003
5. A. Vibhute, T. Patil, R. Gambhir and A.P. Tiwari, *Appl. Surface Sci. Adv.*, **11**, 100311 (2022); https://doi.org/10.1016/j.apsadv.2022.100311
6. K. Rovina, S. Siddiquee and S.M. Shaarani, *Crit. Rev. Anal. Chem.*, **47**, 309 (2017); https://doi.org/10.1080/10408347.2017.1287558
7. K. Hebbache, N.A. Ahmed, N. Aliouane, C. Chassigneux and M. Eyraud, *Microchem. J.*, **213**, 113867 (2025); https://doi.org/10.1016/j.microc.2025.113867
8. N.Y. Stozhko, E.I. Khamzina, M.A. Bukharinova and A.V. Tarasov, *Sensors*, **22**, 4092 (2022); https://doi.org/10.3390/s22114092
9. S. Manzoor, A.H. Dar, K.K. Dash, V.K. Pandey, S. Srivastava, I. Bashir and S.A. Khan, *Appl. Food Res.*, **3**, 100263 (2023); https://doi.org/10.1016/j.afres.2023.100263

10. J. Zhou, W. Nie, Y. Chen, C. Yang, L. Gong, C. Zhang, Q. Chen, L. He and X. Feng, *Food Chem.*, **256**, 304 (2018); https://doi.org/10.1016/j.foodchem.2018.02.002
11. B.B. Campos, R. Contreras-Cáceres, T.J. Bandosz, J. Jiménez-Jiménez, E. Rodríguez-Castellón, J.C.G.E. da Silva and M. Algarra, *Sens. Actuators B Chem.*, **239**, 553 (2017); https://doi.org/10.1016/j.snb.2016.08.055
12. R. Boggia, M. C. Casolino, V. Hysenaj, P. Oliveri and P. Zunin, *Food Chem.*, **140**, 735 (2013); https://doi.org/10.1016/j.foodchem.2012.11.020
13. A. Jain, A. Chaurasia and K.K. Verma, *Talanta*, **42**, 779 (1995); https://doi.org/10.1016/0039-9140(95)01477-S
14. S. Jafari, J. Guercetti, A. Geballa-Koukoula, A.S. Tsagkaris, J.L.D. Nelis, M.-P. Marco, J.-P. Salvador, A. Gerssen, J. Hajslova, C. Elliott, K. Campbell, D. Migliorelli, L. Burr, S. Generelli, M.W.F. Nielen and S.J. Sturla, *Foods*, **10**, 1399 (2021); https://doi.org/10.3390/foods10061399
15. P.K. Yadav, V.K. Singh, S. Chandra, D. Bano, V. Kumar, M. Talat and S.H. Hasan, *ACS Biomater. Sci. Eng.*, **5**, 623 (2019); https://doi.org/10.1021/acsbiomaterials.8b01528
16. P. Nath, K. R. Mahtaba, and A. Ray, *Sensors*, **23**, 5053 (2023); https://doi.org/10.3390/s23115053
17. H. Li, X. He, Z. Kang, H. Huang, Y. Liu, J. Liu, S. Lian, C.H.A. Tsang, X. Yang and S.T. Lee, *Angew. Chem. Int. Ed.*, **49**, 4430 (2010); https://doi.org/10.1002/anie.200906154
18. N. Gogoi, M. Barooah, G. Majumdar and D. Chowdhury, *ACS Appl. Mater. Interfaces*, **7**, 3058 (2015); https://doi.org/10.1021/am506558d
19. M.B. Cánchig, F. López, Z. Morales-Navarro, A. Debut, K. Vizuete, T. Terencio, M. Caetano and J.P. Saucedo-Vázquez, *Carbon Trends*, **18**, 100445 (2025); https://doi.org/10.1016/j.cartre.2024.100445
20. L. Dewangan, Y. Chawre, J. Korram, I. Karbhal, R. Nagwanshi, V. Jain and M.L. Satnami, *Microchem. J.*, **182**, 107867 (2022); https://doi.org/10.1016/j.microc.2022.107867
21. Y. Wei, L. Chen, S. Zhao, X. Liu, Y. Yang, J. Du, Q. Li and S. Yu, *Front. Mater. Sci.*, **15**, 253 (2021); https://doi.org/10.1007/s11706-021-0544-x
22. P. Kumar, S. Dua, R. Kaur, M. Kumar and G. Bhatt, *RSC Adv.*, **12**, 4714 (2022); https://doi.org/10.1039/D1RA08452F
23. J. Tang, J. Zhang, Y. Zhang, H. Xu, Y. Chen and X. Li, *Nanoscale Res. Lett.*, **14**, 241 (2019); https://doi.org/10.1186/s11671-019-3079-7
24. M. Zhang, X. Long, Y. Ma and S. Wu, *Opt. Mater.*, **135**, 113311 (2023); https://doi.org/10.1016/j.optmat.2022.113311
25. K.G. Nguyen, I.A. Baragau, R. Gromicova, M. Culea, I. Stamatin, M. Al-Kassab and M.H. Phan, *Sci. Rep.*, **12**, 13806 (2022); https://doi.org/10.1038/s41598-022-16893-x
26. P. Wu, W. Li, Q. Wu, Y. Liu and S. Liu, *RSC Adv.*, **7**, 44144 (2017); https://doi.org/10.1039/C7RA08400E
27. Z.X. Liu, Z.L. Wu, M.X. Gao, H. Liu and C.Z. Huang, *Chem. Commun.*, **52**, 2063 (2016); https://doi.org/10.1039/C5CC08635C
28. G. Zhang, S. Feng, R. Ge, Y. Liu, and Q. Zhu, *J. Fluoresc.*, **35**, 8189 (2025); https://doi.org/10.1007/s10895-025-04161-w
29. P. Zuo, Z. Chen, F. Yu, J. Zhang, W. Zuo, Y. Gao and Q. Liu, *RSC Adv.*, **10**, 32919 (2020); https://doi.org/10.1039/D0RA04228E
30. D. Bano, V. Kumar, V. K. Singh, and S. H. Hasan, *New J. Chem.*, **42**, 5814 (2018); https://doi.org/10.1039/C8NJ00432C
31. T. Mohanta, H. G. Behuria, S. K. Sahu, A. K. Jena and S. Sahu, *Analyst*, **48**, 5597 (2023); https://doi.org/10.1039/d3an01609a
32. D. Zheng, A. Li, M. Zhang, X. Wang, B. Wu, P. Zhao, X. Jia, J. Ding, Q. Zou and L. Zhu, *Nanoscale*, **12**, 12773 (2020); https://doi.org/10.1039/D0NR01882A
33. C.H. Ravikumar, V. Nair G., M.P. Raghavendra, W. Surareungchai, A. Thakur and R.G. Balakrishna, *New J. Chem.*, **45**, 5890 (2021); https://doi.org/10.1039/D1NJ00199J
34. S. Gao, Y. Chen, H. Fan, X. Wei, C. Hu, L. Wang and L. Qu, *J. Mater. Chem. A Mater. Energy Sustain.*, **2**, 6320 (2014); https://doi.org/10.1039/c3ta15443b
35. H. Xu, X. Yang, G. Li, C. Zhao and X. Liao, *J. Agric. Food Chem.*, **63**, 6707 (2015); https://doi.org/10.1021/acs.jafc.5b02319
36. S.T. Huang, Y. Shi, N.B. Li and H.Q. Luo, *Chem. Commun.*, **48**, 747 (2012); https://doi.org/10.1039/C1CC15959C
37. K. Deng, C. Li, X. Li and H. Huang, *J. Electroanal. Chem.*, **780**, 296 (2016); https://doi.org/10.1016/j.jelechem.2016.09.040